GA–A22744

BASELINE DESIGN OF A MULTI-CHANNEL INTERFEROMETER AND POLARIMETER SYSTEM FOR DENSITY MEASUREMENTS ON ITER

by
T.N. CARLSTROM, R.T. SNIDER, C.B. BAXI,
C.L. RETTIG, and W.A. PEEBLES

NOVEMBER 1997

DISCLAIMER

GA–A22744

BASELINE DESIGN OF A MULTI-CHANNEL INTERFEROMETER AND POLARIMETER SYSTEM FOR DENSITY MEASUREMENTS ON ITER

by
T.N. CARLSTROM, R.T. SNIDER, C.B. BAXI,
C.L. RETTIG,* and W.A. PEEBLES*

This is a preprint of a paper presented at the Workshop for Diagnostics for ITER, September 4–12, 1997, Varenna, Italy and to be published in the *Proceedings.*

*University of California, Los Angeles, California.

Work supported by
the U.S. Department of Energy under
Contract No. DE-AC03-94SF20282 and
Grant Nos. DE-FG03-86ER53266 and DE-FG03-86ER53225

GA PROJECT 3994
NOVEMBER 1997

BASELINE DESIGN OF A MULTI-CHANNEL INTERFEROMETER AND POLARIMETER SYSTEM FOR DENSITY MEASUREMENTS ON ITER

T.N. Carlstrom, R.T. Snider, C.B. Baxi, C.L. Rettig,* and W.A. Peebles*

General Atomics
P.O. Box 85608
San Diego, CA 92186-5608

*University of California, Los Angeles
Los Angeles, CA

ABSTRACT

A design of a multi-channel system to measure line average plasma density for ITER has been developed using vibration compensated interferometry and Faraday rotation measurements. The purpose of this study is to establish a consistent design based on current technology, that can be used to examine performance and reliability issues and to evaluate the effect of future design improvements. The system uses a vibration compensated interferometer, with a CO_2 laser at 10.6 μm for the probe beam and a CO laser at 5.2 μm for the vibration compensation. The CO_2 laser probe beam also allows Faraday rotation measurements to be made along the tangential beam path. This improves the reliability of the system because density measurements made from the Faraday rotation, although less accurate than interferometry, do not require cumulative knowledge of the phase shift over the long time scales expected in ITER. Plasma effects on both types of measurements and ITER specific operational considerations, such as plasma start-up, pulse length, and vibration effects will be discussed. Survivability and placement of the plasma facing optics in the ITER structure are critical issues and a discussion of the material selection, and integration into the ITER design are given.

1. INTRODUCTION

The electron density measurement is expected to play a critical role in the operation of ITER and in the basic understanding of the ITER plasmas. The avoidance of density limit disruptions, burn control and fueling all require accurate active density feedback control.[1] While active density feedback control is routinely used in present day tokamaks, the size, environment and pulse length of ITER places new constraints and requirements on a density control diagnostic. The severity and possible consequences of disruptions are of particular concern when considering the reliability of a density control diagnostic. The critical nature of the density measurement has lead us to a design using laser interferometry techniques with adequate density accuracy and that have proven to be robust and reliable for density control in other tokamaks. In the ITER baseline design presented here, a short wavelength probing laser beam is used both as an interferometer to measure line average

electron density and as a polarimeter to measure the plasma induced Faraday rotation which is proportional to $\int n_{e(z)} B(z) dz$.[2] The addition of the Faraday rotation measurement improves the reliability of the overall system, particularly during long pulse operation, since the phase rotation is less then 2 π and hence does not have to rely on keeping track of a cumulative fringe count during the entire pulse. The line averaged density measured with Faraday rotation can be used to check and correct any counting errors that may occur in the higher resolution interferometer measurement.

Previous studies have shown that a vibration compensated interferometer system based on a CO_2 laser is near optimum for ITER in terms of refraction, density resolution, plasma facing optics survival and access to ITER.[3,4] Here we describe the ITER baseline design of the density measurement system based on a vibration compensated CO_2 interferometer and polarimeter using existing technology that we believe meets the needs of ITER. This baseline design which self consistently fits all of the major components together, can then be used to benchmark and test future design improvements or new concepts.

2. ITER INTERFEROMETER/POLARIMETRY BASELINE DESIGN

System Layout

A plan view of ITER showing five tangential probe beam paths through the ITER plasma is shown in Fig. 1. This geometry was chosen over radial or vertical viewing systems because of the severe access constraints on ITER.[4] A radial system for example requires optical surfaces on the center, inside wall of the torus where neutron streaming to the inner TF coils prevent adequate penetrations through the inner shield modules for mirrors. The five beams shown in Fig. 1 provide coverage for the various stages during the plasma growth as shown in Fig. 2 and give some crude real-time density profile information. Work by Bower has shown that these few interferometer channels combined with an edge reflectometer can provide density profiles with good spatial resolution throughout the plasma.[5] The multiple beam paths also improve the reliability of the entire diagnostic by giving some redundancy during the flattop portion of the plasma pulse.

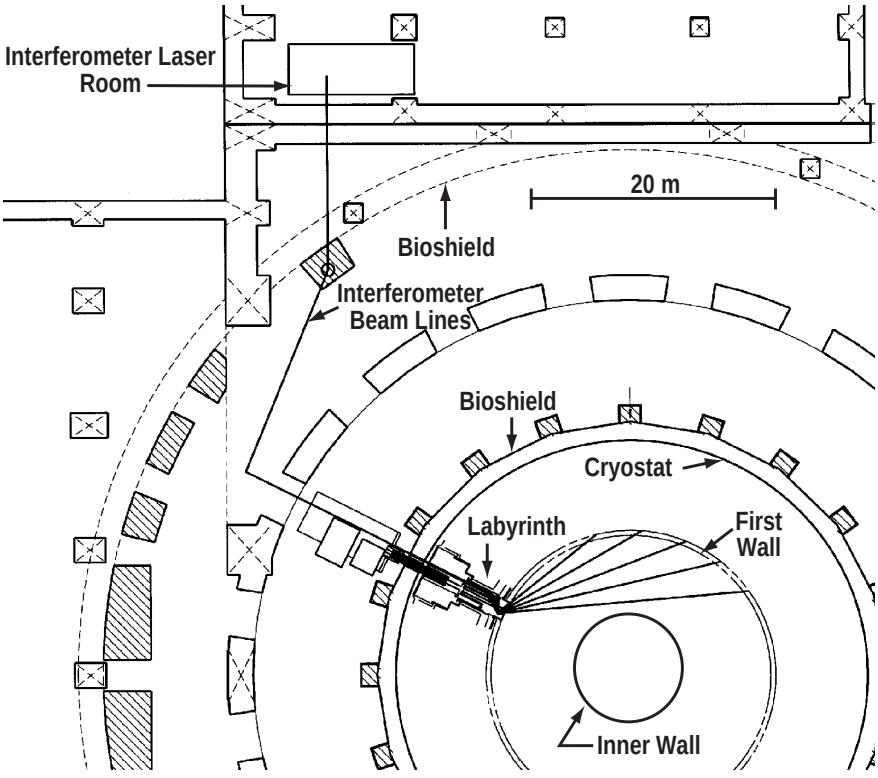

Figure 1. Plan view of ITER and proposed beam paths and laser room.

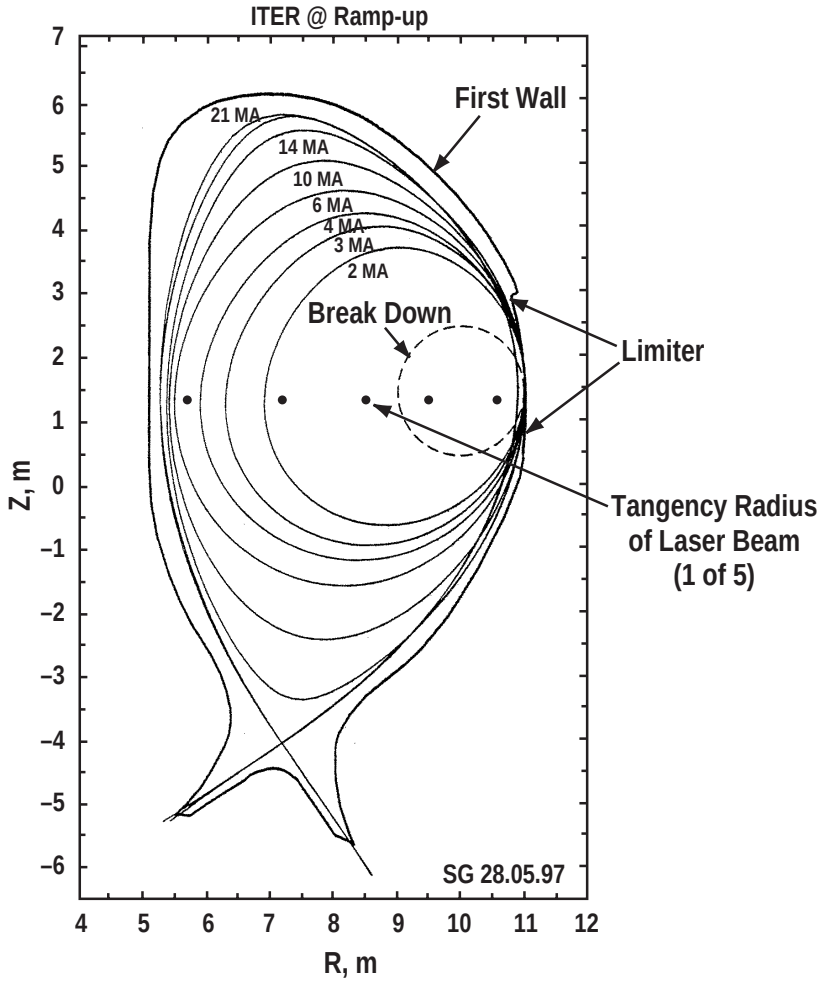

Figure 2. Cross section of ITER and the current plasma startup scheme along with the tangency radius of the five laser beam paths.

All five of the laser beam paths enter and exit the plasma chamber from a single port and are reflected back down the same beam path (with an offset) by retroreflectors embedded behind the ITER shield modules. A plan view of the beam paths through the port shield plug are shown in Fig. 3. By requiring only a single port with no large vibration damping structure the total penetration area through the shield modules is minimized and the neutron leakage both to the bioshield and to the TF coils is kept small thus reducing the total external shielding required.

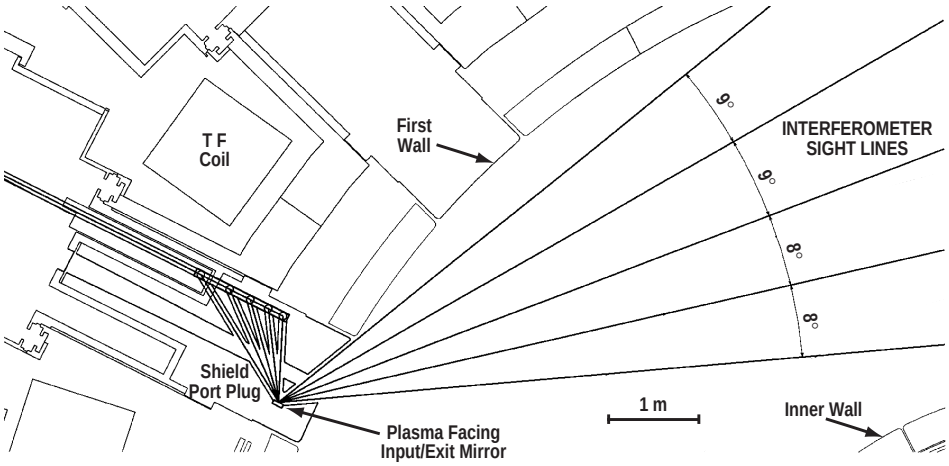

Figure 3. Plan view of the input/exit port plug and laser beam paths.

The optical path through the shield plug on the entrance/exit port forms a labyrinth in order to reduce the escaping neutrons to acceptable levels. The retroreflectors are recessed in the shield wall to minimize their exposure to the plasma and neutrons as shown in Fig. 4. All of the optical components within the bioshield of ITER are reflective except for the vacuum windows which are well behind the port plug and in a relatively benign radiation environment. Reflective optics were chosen to avoid neutron damage issues associated with transmission optics.

Each beam path has collinear 10.6 μm (CO_2) and 5.3 μm (CO) laser probe beams. This choice of laser wavelengths has acceptable refraction and phase resolution[3,4] and commercial laser detector combinations with good power/sensitivity are available. The tokamak community has experience with both CO_2 and CO laser interferometer systems.[8–11]

The interferometer portion of the diagnostic uses standard two color heterodyne interferometry using acousto-optic modulators (Bragg cells) to generate the intermediate frequency (IF). The Bragg cells shown in Fig. 5, split the incoming laser beam into two beams separated by a small angle with one beam at the initial frequency (ω) and the other at the initial frequency plus the modulator frequency (ω + 42 MHz for example). Figure 5 shows a schematic layout of both arms of the two colors (CO_2 and CO laser wavelengths). To make the Faraday rotation measurement right and left circularly polarized beams at different frequencies are generated from a single CO_2 laser beam and recombined to produce an elliptically polarized beam which rotates at half the difference frequency. The rotating elliptical beam is passed through the plasma and allowed to interfere with a reference beam at a single detector as shown in Fig. 5(a). The output from the detector is then split, filtered and the phase detected (relative to the IF frequencies) as shown in Fig. 5(b). This method is currently used with FIR laser systems in TEXTOR[12] and RTP[13] and can be extended for use with a CO_2 laser system. The signals from the phase detectors shown in Fig. 5(b) can be used to extract the line average electron density using both the CO and CO_2 interferometer signals to measure and subtract the phase shift induced by vibrations or motion of the mirrors ($\phi_{vib}=2\pi\Delta L/\lambda$ where ΔL is the motion of the mirrors in the direction of the beam) from the phase shift induced by the plasma density ($\phi_{nel}=2.8\times10^{-15}\lambda \int n(z)dz$). A signal from the same CO_2 detector can be used to measure the Faraday rotation angle, $\alpha_F=2.6\times10^{-13}\lambda^2 \int n_{el}(z)B(z)dz$.

This method for making the interferometer and Faraday rotation measurements requires a minimum of detectors (one CO_2 and one CO detector for each spatial channel), uses separate CO_2 and CO lasers for each spatial channel, and has no mechanically moving parts such as rotating grating or polarization rotator. In addition, all of the required components are commercially available. This combination of attributes helps assure that the system will be robust and reliable. The high modulation frequency (4 MHz in Fig. 5) permits the system to follow rapid changes in the density without loss of accuracy.

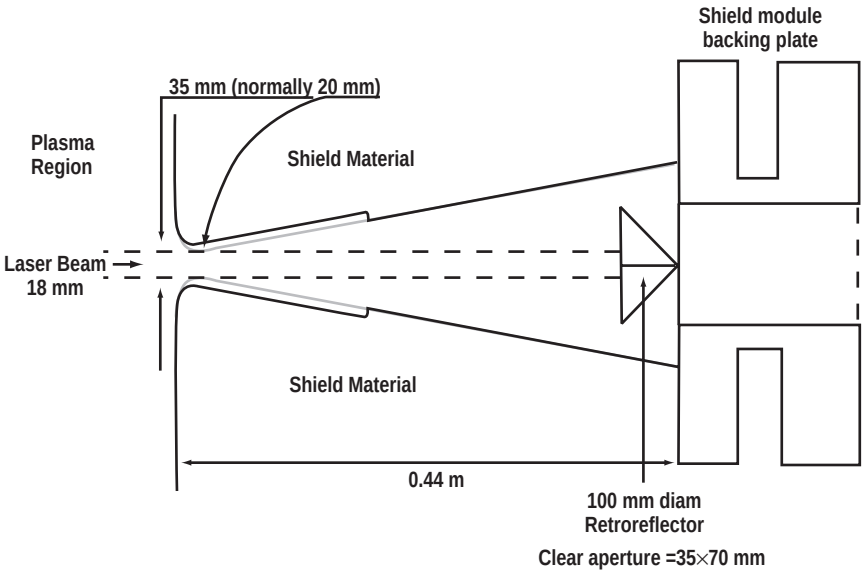

Figure 4. Elevation view of a retroreflector behind the shield modules in the space between modules.

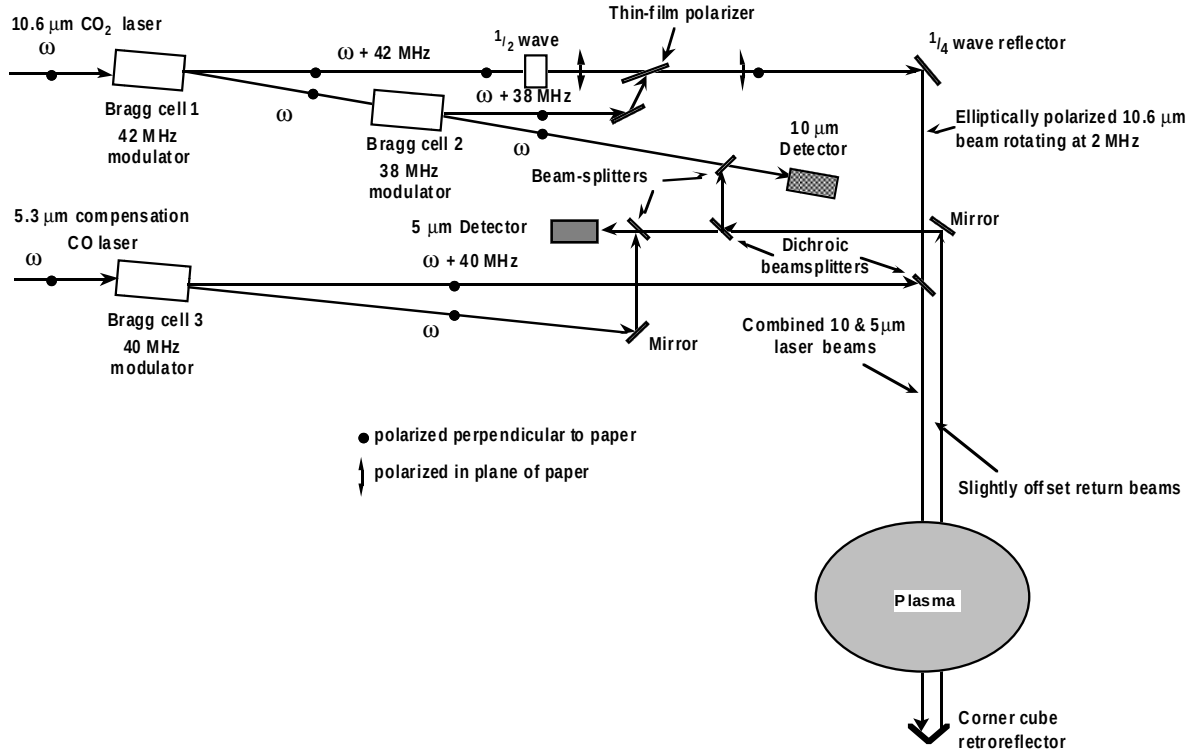

Figure 5(a). Schematic layout of the vibration-compensated interferometer (CO and CO_2 lasers) and the additional Bragg cell and polarizers for making the elliptically polarized CO_2 laser beam for the Faraday rotation measurement.

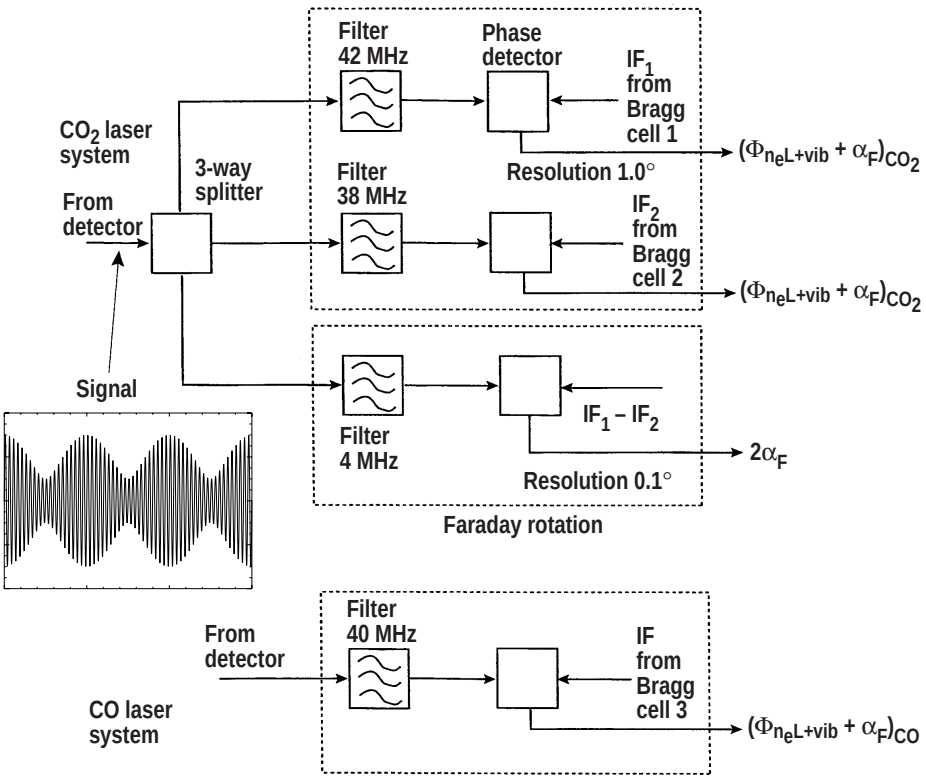

Figure 5(b). The signal from a single CO_2 detector is split and filtered to give three signals that can be used to calculate $\int n_e dz$ and $\int n_{e(z)} B(z) dz$ The signal from the CO detector is used to subtract the phase shift due to vibrations of the mirrors.

Beam Path Layout

We have done an approximate Gaussian beam optics calculation to estimate the laser beam size along a typical beam path as shown in Fig. 6. We start with a near diffraction limited CO_2 laser beam (DEOS[14] LC-40, 40 W, 1.54 mm output beam diameter, full angle divergence θ=9.7 mrad; diffraction limit $\theta = 4\lambda/\pi d_0$ = 8.8 mrad), which is then 3× expanded and focused to a beam waist 2 m away. This keeps the beam diameter small, between 4.62 mm and 6.46 mm, while on the optics table where it passes through two Bragg cells, several retardation reflectors, mirrors, and beam combiners. A typical Bragg cell (IntraAction[15] AGM-406) has an aperture of 6 mm and power density capability of 320 W/cm^2. These specifications are easily met if the Bragg cells are placed near the first beam expander. The resulting beam is further expanded by 3.6× before it is combined with the CO laser beam and leaves the optics table to start its path to the plasma. At this point, the beam diameter is 23.2 mm and the divergence is 0.9 mrad. The CO laser beam is handled in a similar manner so that it has approximately the same beam diameter and divergence. An 18.0 mm beam waist is formed about 20 m from the beam expander and this beam waist is relayed to the position of the corner cube by a focusing mirror located midway between these two positions. The return beam is offset horizontally 35 mm at the corner cube (clear aperture 35×70 mm), and returns through the same optics as the incident beam. This offset is required to prevent the return beam from re-entering the laser and affecting its stability. Due to the relay optics, the return beam has the same diameter as the incident beam. At the optics table the beam is combined with the reference CO_2 and CO laser beams and focused on the detectors.

There are several possibilities for feedback alignment control. In Fig. 6 we show a CO_2 beam position sensor before the second alignment mirror, close to the vacuum window. This sensor is used to control the first alignment mirror so the beam is properly located at the vacuum window. The second CO_2 beam position sensor is located at the optics table, just before the beam is combined with the reference beams. This sensor is used to control the second alignment mirror, and keeps the beam focused on the detector. The CO beam is made collinear with the CO_2 beam using a similar method (not shown in Fig. 6). To

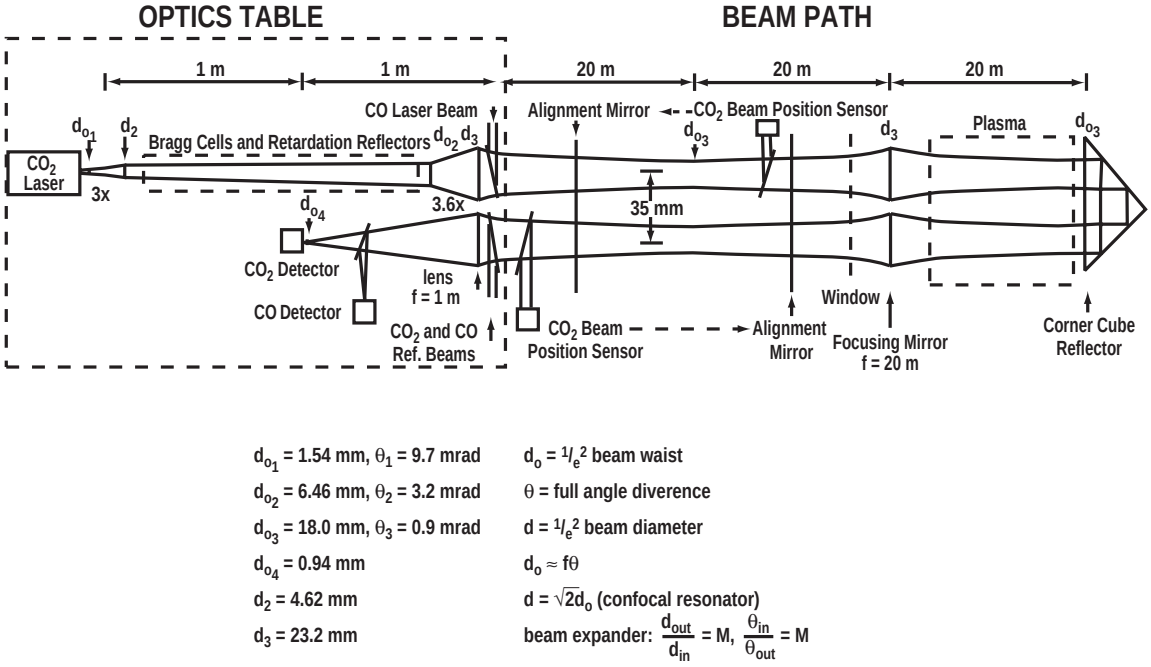

d_{o_1} = 1.54 mm, θ_1 = 9.7 mrad
d_{o_2} = 6.46 mm, θ_2 = 3.2 mrad
d_{o_3} = 18.0 mm, θ_3 = 0.9 mrad
d_{o_4} = 0.94 mm
d_2 = 4.62 mm
d_3 = 23.2 mm

$d_o = 1/e^2$ beam waist
θ = full angle diverence
$d = 1/e^2$ beam diameter
$d_o \approx f\theta$
$d = \sqrt{2}d_o$ (confocal resonator)
beam expander: $\frac{d_{out}}{d_{in}} = M$, $\frac{\theta_{in}}{\theta_{out}} = M$

Figure 6. An estimate of the beam diameter along the entire beam path using Gaussian beam optics. Note that the vertical and horizontal scales are different and not to scale.

maintain a good interference signal, the beam splitter that combines the plasma and reference beams can be dithered in a feedback alignment scheme to give the maximum interference signal (38–42 MHz).

The plasma facing mirrors (one steering mirror and three corner cube mirrors) are made from tungsten, whose reflectivity is about 70% at these wavelengths. The five reflections from these mirrors reduce the laser power to 17%. Assuming the transmission of 20% for the rest of the optics (30 reflections at 95%), a 30 W CO_2 laser would produce about 1 W at the detector. This is adequate for room temperature detectors. Cooled detectors have about 100 times improved detectabilty, so signal levels should not be an issue.

Estimate Of Signals And Errors

An estimate of the phase shift and Faraday rotation angle from a central viewing channel for a normal ITER plasma discharge[6] is shown in Fig. 7. Small variations of the laser wavelength will result in a vibration compensation error that is proportional the change in path length due to mirror motion. This error is anticipated to be larger than the phase measurement error (assumed to be 1°) because of the large (2 cm) motion of the vacuum vessel of ITER during the discharge. Experience from DIII–D[4] suggests that the amount of vibration will be proportional to the OH coil flux, shown in Fig. 7(b). The phase shift due to the expected mirror motion is shown in Fig. 7(e) and Fig. 7(f) shows the resulting error in the density measurement for a 250 MHz variation in the laser frequency (typical of commercial lasers). The last two plots in Fig. 7 display the Faraday rotation angle for the ITER discharge and the uncertainty based on a phase detection error of 0.1°. The expected errors throughout the discharge are well within the ITER requirements.[6] The error in the Faraday rotation measurement during the flattop is less then 1%. This very low error, if realized, suggests that the Faraday rotation measurement from this system has the accuracy to make a measurement of the internal diamagnetism of the plasma as described in Ref. 3.

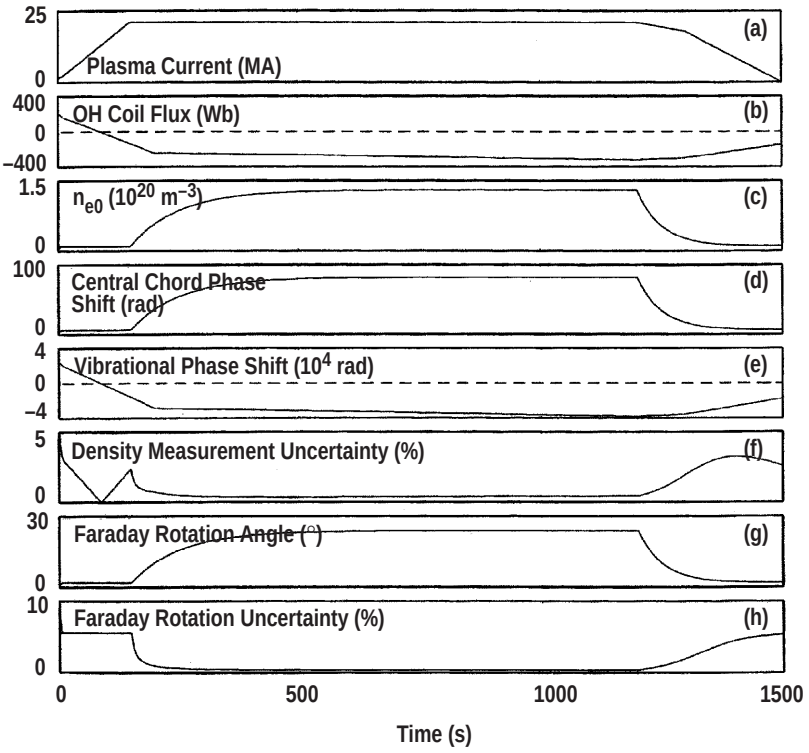

Figure 7. Time traces of plasma parameters and density measurements signals.

3. PLASMA FACING MIRRORS

A major concern for any optical diagnostic on ITER is the survivability of the plasma facing optical components. Surface roughness and distortion of the flat mirror should be kept below 1.2 μm (λ/4 for 5 μm) to maintain the phase fronts of the probing beams. A further requirement for the retroreflectors is that the perpendicularity of the three flat surfaces that make up the retroreflector must be maintained to less then 10 arc sec corresponding to a 1 mm shift in the return beam at the input/exit port.

A finite element thermal analysis code was used to calculate the distortion of water-cooled tungsten mirrors for a full power steady-state ITER discharge. Thermal distortion of the mirrors due to non-uniform heating from plasma radiation and neutrons is less then 0.9 μm as shown in Table 1. A refined water cooling design and minor change in the geometry of the mirrors reduced the thermal distortion of these mirrors from that reported in Ref. [3]. The change in perpendicularity of the retroreflectors due to thermal distortion from plasma and neutron heating is calculated to be less then 4 arc sec.

Sputtering from charge exchange neutrals does not appear to be an issue for the tungsten mirrors with the geometry shown in Fig. 1. An estimate of the CX sputtering rates for the input/exit mirrors is shown in Table 2. The calculations and assumptions from which this estimate were made follow the work done by Mayer and de Kock.[16] We assume a CX-flux (Γ_{tot}) of 2×10^{19} atoms m^{-2} s^{-1} hitting the walls of ITER and that the flux incident on the mirrors is $\Gamma_{mirror}= \Omega/\pi\ \Gamma_{tot}$ where Ω is the solid angle of the plasma as viewed by the mirror. The flux consists of 50% D and 50% T and the energy distribution of the neutrals (both D and T) were taken from Fig. 2 in Ref. 16. The mirrors for the interferometer are not normal to the plasma surface and an increase in the sputtering erosion of up to $\cos^{-f}\Theta$ can result, where $1 < f < 2$ and Θ is the angle of incidence.[17] Because of this effect, the erosion rates have been increased by a factor of two over the values calculated from the normal incident sputtering yields. As shown in Table 2, the estimated erosion from sputtering during the lifetime of ITER[7] is well below the 1.2 μm required for operation of the diagnostic for tungsten, rhodium, and molybdenum mirrors.

The plasma facing optics in the present design have anticipated thermal distortion and sputtering levels that are acceptable. The key to reducing both the sputtering and the thermal distortion is the choice of materials (with tungsten as the clear favorite), the cooling geometry, and the minimization of the solid angle view of the plasma by the optics.

Table 1. Finite element thermal/stress analysis results for the plasma facing mirrors. Distortion is below the required 1.2 μm. The water flow velocity in the cooling channels was adjusted to give reasonable temperature and distortion.

	Maximum Distortion	Plasma Radiation Heat Load	Neutron Heating	Water Flow Velocity	Temperature Variation Across Surface
Flat input/exit mirror	0.9 μm	4.95 W/cm^2	4.2 W/cm^3	10 m/s	8°C
Retroreflector	0.36 μm	0.09 W/cm^2	0.36 W/cm^3	1 m/s	5°C

Table 2. Calculated maximum sputtering removal rates for the flat input/exit mirror. Tungsten, Rhodium and Molybdenum have removal rates that will allow the mirror to survive (less than 1.2 μm of materials removed) the life of ITER.

Mirror Material	Sputtering Removal Rate (μm/s)	Material Removal per ITER Shot	Material Removal During Expected ITER Life
Tungsten	1.3×10^{-9}	1.3×10^{-6} μm	0.13 μm
Rhodium	2.2×10^{-9}	2.2×10^{-6} μm	0.22 μm
Molybdenum	5.3×10^{-9}	5.3×10^{-6} μm	0.53 μm
Copper	4.4×10^{-8}	4.4×10^{-5} μm	4.4 μm

While these results have reasonable safety margins, significant increases in the plasma radiated power (factors of two or more) over the estimates used in the calculations could result in thermal distortion problems. A remaining unaddressed issue is coating of the optics from the plasma. Anecdotal information from existing tokamaks suggest that if the optical component is recessed from the first wall by more then one or two diameters of the penetration through the wall then coating of optics is minimal. While the present design satisfies that criteria the very long pulse length of ITER may require other ways to reduce the plasma coating. Systematic studies in present day tokamak should be able to better address this issue.

4. DISCUSSION

Knowledge of the electron density is important for the control of the plasma and safety of the tokamak. Therefore, the interferometer system must be robust and have suitable redundancy and reliability. In this regard, we recommend that the five chords of the proposed interferometer be independent systems, each with their own lasers, optics, detectors and electronics. Only a few common elements of the beam path, such as the final plasma facing turning mirror should be shared. (Even the plasma facing mirror could be made separate for each spatial channel, however there is a significant penalty to be paid in terms of port space and neutron streaming). This would offer significant redundancy, insuring that at least one interferometer is always operational. All electronic and delicate components should be located in an area where personnel access is permitted and an inventory of spare parts maintained.

We have chosen to avoid the use of mechanical polarization rotators or frequency shifters in favor of solid state acousto-optic modulators. We feel the solid state technology offers much higher reliably. For this same reason, we have chosen not to pursue efficient designs that use a rotating grating to produce multiple chords from a single laser beam.[18,19]

In summary, we have developed a baseline design for an interferometer and polarimetry density measurement for ITER that meets the ITER requirements both in terms of performance of the diagnostic and integration into the ITER device. The design uses well established techniques and components and should be viewed as a measure for future improvements or new concepts for density measurements. Future work includes a demonstration of a complete system on an existing tokamak, detailed neutronics calculations to verify the rough calculations to date, systematic studies on window coatings by tokamak plasmas and a detailed design of the optical system including the alignment system.

ACKNOWLEDGMENTS

We wish to thank C. Walker and N. Kobayashi of the ITER Joint Central Team for the machine drawings of ITER. This work supported by U.S. Department of Energy under Contract No. DE-AC03-94SF20282 under Raytheon Engineers & Constructors, Inc., Subcontract No. ITER-GA-4002.

REFERENCES

1. ITER Report TAC-95-15; TAC-JCT informal technical reviews.
2. F.C. Jobes and D.K. Mansfield, Rev. Sci. Instrum. **63**, 5154 (1992).
3. R.T. Snider, et al., Proceedings of the International Workshop on Diagnostics for ITER. Plenum Press, 225 (1996).
4. R.T. Snider, et al., Rev. Sci. Instrum. **68**, 728 (1997).
5. D. Brower, et al., submitted to Plasma Physics and Controlled Fusion.
6. A.E. Costley, et al., Proceedings of the International Workshop on Diagnostics for ITER. Plenum Press, 23 (1996).
7. Dv. Orlinski, Ibid p 51.
8. T.N. Carlstrom, D.R. Ahlgren, and J. Crosbie, Rev. Sci. Instrum. **59**, 1063 (1988).
9. Y. Kawano, et al., Rev. Sci. Instrum. **63**, 4971 (1992).

10. J.H. Irby, et al., Rev. Sci. Instrum. **59**, 1568 (1988).
11. P. Innocente, S. Martini, Rev. Sci. Instrum. **63**, 4996 (1992).
12. H. Soltwisch, "Combined interferometric and polarimetric diagnostics for TEXTOR," Jülich Report Jul-1638 (1980).
13. J. Rommers, Ph.d. Thesis, FOM-Instituut voor Plasmafysica, Nieuwegiun.
14. DEOS, 1280 Blue Hills Avenue, Bloom Field, Connecticut
15. IntraAction Corporation, 3719 Warren Avenue, Bellwood, Illinois.
16. M. Mayer and L. deKock, CX Erosion of Mirrors, IPP Report in progress.
17. E.W. Thomas, Atomic Data for Controlled Fusion Research, Vol. III, "Particle Interactions with Surfaces," ORNL-6088/V3 (1985).
18. J. Howard, Rev. Sci. Instrum. **61**, 1086 (1990).
19. F.C. Jobes, Rev. Sci. Instrum. **66**, 386 (1995).